Japanese Journal of Applied
Physics

The Japan Society
of Applied Physics

Research & Developments for Millimeter-Wave Dielectric Forsterite with Low Dielectric Constant, High *Q*, and Zero Temperature Coefficient of Resonant Frequency

To cite this article: Tsutomu Tsunooka *et al* 2013 *Jpn. J. Appl. Phys.* **52** 09KH02

Japanese Journal of Applied Physics **52** (2013) 09KH02
http://dx.doi.org/**10.7567/JJAP.52.09KH02**

REGULAR PAPER

Research & Developments for Millimeter-Wave Dielectric Forsterite with Low Dielectric Constant, High *Q*, and Zero Temperature Coefficient of Resonant Frequency

Tsutomu Tsunooka[1], Minato Ando[1], Sadahiko Suzuki[2], Yoshitoyo Yasufuku[3], and Hitoshi Ohsato[1,4*]

[1] *Incubation Center, Nagoya Institute of Technology, Nagoya 466-8555, Japan*
[2] *Marusu-Glaze Co., Ltd, Seto, Aichi 489-0032, Japan*
[3] *Yasufuku Ceramics Co., Ltd., Okazaki, Aichi 444-0838, Japan*
[4] *Department of Research, Nagoya Industrial Science Research Institute, Nagoya 464-0819, Japan*
E-mail: ohsato.hitoshi@nitech.ac.jp

Received May 27, 2013; accepted June 25, 2013; published online September 20, 2013

Forsterite Mg_2SiO_4 is a candidate for millimeter-wave dielectrics because of its high Q and low dielectric constant ε_r. Commercial forsterite has been improved with a high Q of 240,000 GHz using high-purity and fine raw materials, and the temperature coefficient of resonant frequency (*TCf*) can also be adjusted to near-zero ppm/°C by adding 24 wt % rutile compared with that in a previous study. In this study, the *TCf*, $TC\varepsilon$, and ε_r of forsterite ceramics with rutile added are studied for the tuning conditions. Zero ppm/°C *TCf* of the forsterite with 30 and 25 wt % rutile added was achieved at 1200 °C for 2.5 and 2.25 h, respectively. The ε_r values of the near-zero *TCf* forsterite with 30 and 25 wt % rutile added are 11.3 and 10.2, respectively. © 2013 The Japan Society of Applied Physics

1. Introduction

Millimeter-wave wireless communications with high data transfer rate for non-compressed digital video transmission systems and radar for the pre-crash safety system have been developed recently. These systems for millimeter-wave wireless communications require resonators and substrates with high quality factor (Qf), low dielectric constant (ε_r),[1] and near-zero temperature coefficient of resonance frequency (TCf).[1] They also require other physical properties such as high thermal conductivity and small thermal expansion.[2] Millimeter-wave dielectrics are required to have high Qf because of the high losses at high frequencies, and also low dielectric constants because of the accuracy control in fabrication.[2,3] Since the substrates in a radar system are exposed to a wide range of temperatures inside a narrow space between the front of the engine room and the radiator, the TCf of the substrates should be tuned to near-zero. Ceramic substrates are more superior than resin substrates, because of their high Qf, near-zero TCf, high thermal conductivity, and small thermal expansion.[4] Silicates are suitable for millimeter-wave dielectrics because of their low dielectric constant owing to their crystal structure consisting of silicon tetrahedron SiO_4 with 50% covalency.[2,5–7] Forsterite (Mg_2SiO_4) is one of the silicates that have good dielectric properties, namely, a high Qf of 240,000 GHz, ε_r of 6.8, and TCf of −67 ppm/°C.[1] We have been studying forsterite for a long time.[8] Tsunooka et al. improved Qf from 10,000 GHz of commercial forsterite to 240,000 GHz using high-purity and fine-grain raw materials;[1] their forsterite has no contaminations and no glassy phase among clear grains.[3] Moreover, a Qf of 270,000 GHz has been achieved by adjusting the composition.[9] As TCf is −67 ppm/°C, a TCf of zero ppm/°C was designed by adding rutile (TiO_2) with plus TCf of 450 ppm/°C. However, TCf could not be improved because of the disappearance of rutile due to the too high sintering temperature.[10] When the rutile-added forsterite was sintered at 1200 °C for 2 h, the TCf was zero ppm/°C at 24 wt % rutile added. The millimeter-wave dielectric properties were excellent: $TCf =$ 0 ppm/°C, $Qf =$ 85,000 GHz, and $\varepsilon_r = 11$.[11–14] The sintering temperature was decreased by 150 °C from 1350 to 1200 °C. Rutile has two roles: one is to control TCf at zero, and another is as a sintering agent. The reason for the disappeareance of rutile in high-temperature sintering can be explained on the basis of the $MgO–SiO_2–TiO_2$ ternary phase diagram, as shown in Fig. 1.[15] The composition denoted by X of rutile added-forsterite is located in the compositional triangle of $MgO{\cdot}2TiO_2–2MgO{\cdot}SiO_2–MgO{\cdot}SiO_2$ subsystem. As the composition in the triangle reacts with rutile, and convert to three compounds, namely, $MgO{\cdot}2TiO_2$, $2MgO{\cdot}SiO_2$, and $MgO{\cdot}SiO_2$ according to the following chemical formula, the rutile phase disappears finally.

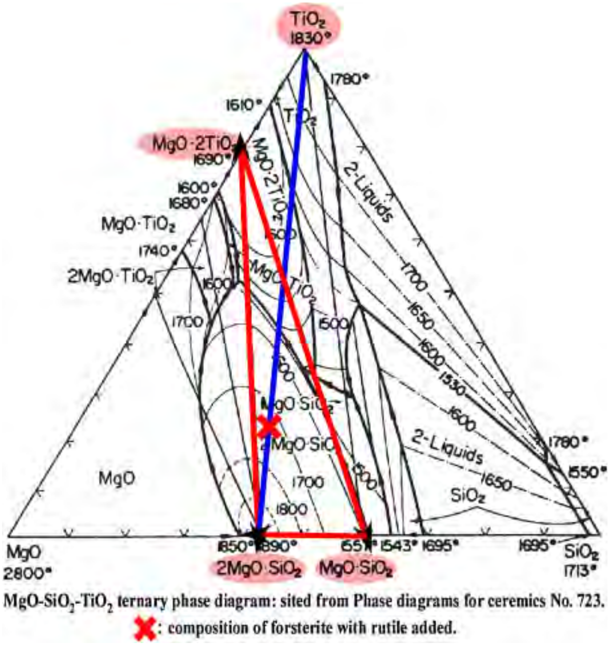

MgO-SiO_2-TiO_2 ternary phase diagram: sited from Phase diagrams for ceremics No. 723.
X: composition of forsterite with rutile added.

Fig. 1. (Color online) $MgO–SiO_2–TiO_2$ ternary phase diagram. The forsterite with rutile added forsterite denoted by X is located in the compositional triangle of the $MgO{\cdot}2TiO_2–2MgO{\cdot}SiO_2–MgO{\cdot}SiO_2$ subsystem.

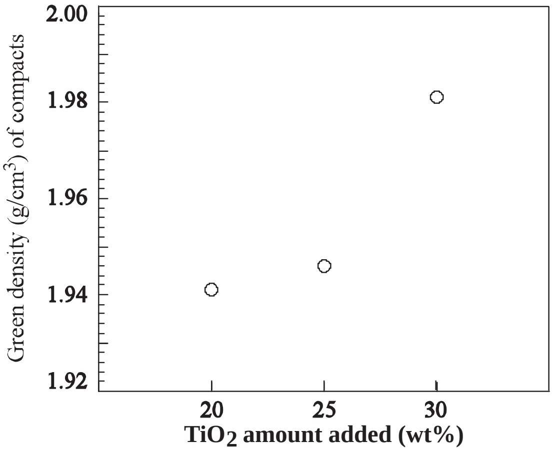

Fig. 2. Green density of compacts as a function of amount of TiO_2 added.

$$Mg_2SiO_4 + xTiO_2 \rightarrow \left(\frac{x}{2}\right)MgTi_2O_5 + xMgSiO_3 + \left(1 - \frac{x}{2}\right)Mg_2SiO_4 \quad (0 < x < 2). \quad (1)$$

In this work, determinations of the tuning conditions *TCf*, *TC*ε, and dielectric constants are performed for the excellent millimeter-wave dielectric forsterite with zero *TCf* for mass production.

2. Experimental Procedure

High-purity (99.9%) and fine particle size of 0.1 µm for MgO and 0.82 µm for SiO_2 powders were weighed by 10 Kg in terms of mole ratio: $MgO : SiO_2 = 2 : 1$. These powders were mixed for 24 h in a polyethylene bottle with 1000 ml of distilled water and 3.2 kg of polyurethane-coated iron balls with a diameter of 15 mm. The mixture was dried and calcined in a high-purity alumina crucible at 1150 °C for 3 h in air.[16,17] The calcined powder, which was pure forsterite phase identified by X-ray powder diffraction (XRPD), was pulverized using a ball mill. The mean particle size was 0.81 µm. Then, high-purity (99.9%) TiO_2 with a fine particle size of 0.25 µm was added so as to prepare samples of three compositions: fotsterite samples with 20, 25, and 30 wt % TiO_2 added denoted as T20, T25, and T30, respectively, (throughout this paper the sample composition is expressed in mass fraction %). These mixtures were pulverized to an average particle size under 1 µm. After addition of the poly(vinyl alcohol) (PVA) organic binder (1 wt %) and wax (1 wt %), a second attrition was carried out to reach a homogeneous distribution with average particle size of about 1 µm. The resultant mixture was obtained as granular powder. The powder was pelletized into cylindrical compacts 12 mm in diameter and 5–7 mm in thickness using a uniaxial press (150 MPa). Figure 2 shows the green density of compacts as a function of the amount of TiO_2 added. The compacts were debindered at 500 °C for 12 h and sintered at 1200 °C as a function of sintering time (1.0, 1.5, 2.0, 2.5, and 3 h). The crystalline phases of sintered pellets were identified by XRPD. After the surface of the specimens was ground and polished, the bulk density was measured by the Archimedes' method. The microstructure was observed from the back-scattering electron images obtained by scanning electron microscopy (SEM). The microwave dielectric properties (ε_r and *Qf*) were measured by Hakki and Coleman's method in the $TE_{01\delta}$ mode using a network analyzer (Agilent 8720ES, JIS R 1627-1996).[18–21] *TCf* was measured in the temperature range between 20 and 80 °C.

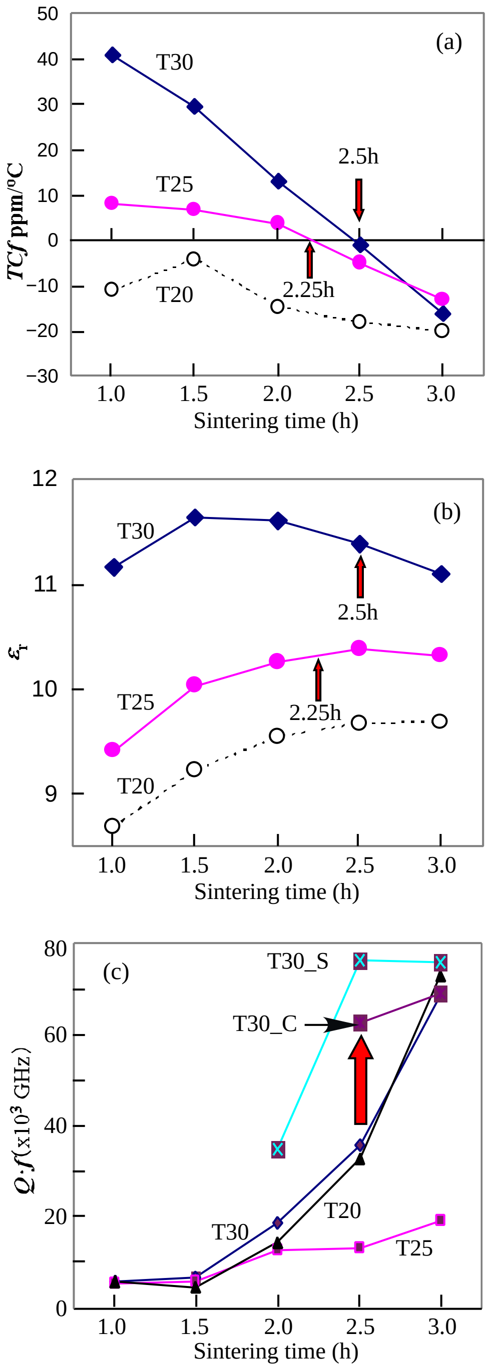

Fig. 3. (Color online) Millimeter-wave dielectric properties of forsterite with 20, 25, and 30 wt % rutile added as a function of sintering time. (a) *TCf*, The arrows show the points of *TCf* = 0 ppm/°C: 2.5 h for T30 and 2.25 h for T25. (b) ε_r, The arrows for 2.5 and 2.25 h show ε_r values of 11.4 for T30 and 10.2 for T25, respectively. (c) *Qf*, The arrows for T30_C and T30_S show improvement of *Qf* from 30,000 GHz to 60,000–80,000 GHz by the polishing of the resonator and powder technology, respectively.

3. Results and Discussion

Figure 3 shows the millimeter-wave dielectric properties of forsterite with 20, 25, and 30 wt % rutile added as a function

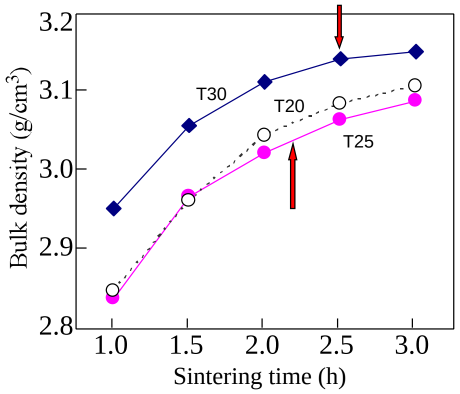

Fig. 4. (Color online) Bulk density of forsterite with 20, 25, and 30 wt % rutile added as a function of sintering time. The arrows for 2.5 and 2.25 h show ε_r values of 11.4 for T30 and 10.2 for T25, respectively.

of sintering time. The sintering temperature is 1200 °C, which is for the remaining rutile phase determined on the basis of the report by Tsunooka et al.[11] The TCf values of forsterite with a much rutile phase are located on the plus side, and TCf decreases with increasing sintering time, as shown in Fig. 3(a). When the sintering time for T30 and T25 is just 2.5 and 2.25 h, respectively, TCf becomes zero ppm/°C. The precise TCf values can be tuned by adjusting sintering time. In the case of T20, TCf could not reach zero ppm/°C because of the small amount of rutile.

Figure 3(c) shows the Qf values of forsterite ceramics; Qf increases from 10,000 to 70,000 GHz with sintering time. The Qf of the T30 sample with $TCf = 0$ ppm/°C sintered for 2.5 h is 30,000 GHz. Qf increases to 80,000 GHz for the different procedures of samples such as powder technology and polishing of the resonator. The Qf of the T25 sample did not increase to more than 20,000 GHz, because of the low green density of green compacts, as shown in Fig. 2, owing to the synthesized forsterite powder shape with the twined particles. The dielectric constant increases with the amount of rutile added as shown in Fig. 3(b). The increase in ε_r at an early stage of sintering depends on bulk density, as shown in Fig. 4. In the second half, the decrease in ε_r depends on the formation of $MgTi_2O_5$ formed by reaction between rutile and MgO dissociated from forsterite. The ε_r value of the T30 sample sintered for 2.5 h is about 11.3, and that of T25 sintered for 2.25 h is about 10.2. The ε_r values can also be tuned by adjusting sintering time and the amount of rutile added. These samples sintered well with densities higher than 3 g/cm^3, as shown in Fig. 4. The reason for the low Qf values of T25 is its lower density than the others samples. Tuning of the temperature coefficient of dielectric constant ($TC\varepsilon$) could be introduced from TCf using the following equation:

$$TC\varepsilon = -2(TCf + \alpha). \tag{2}$$

Here, α is the linear thermal expansion coefficient.[22] The α value of forsterite was 11.3 ppm/°C, which was measured from room temperature to 100 °C. The relationship between TCf and $TC\varepsilon$ is shown in Fig. 5(a). Figure 5(b) shows $TC\varepsilon$ as a function of sintering time, which is derived from TCf using Eq. (2). Zero $TC\varepsilon$ was obtained at 2.8 h for T25 and T30. For T20, the $TC\varepsilon$ values are ±15 ppm/°C.

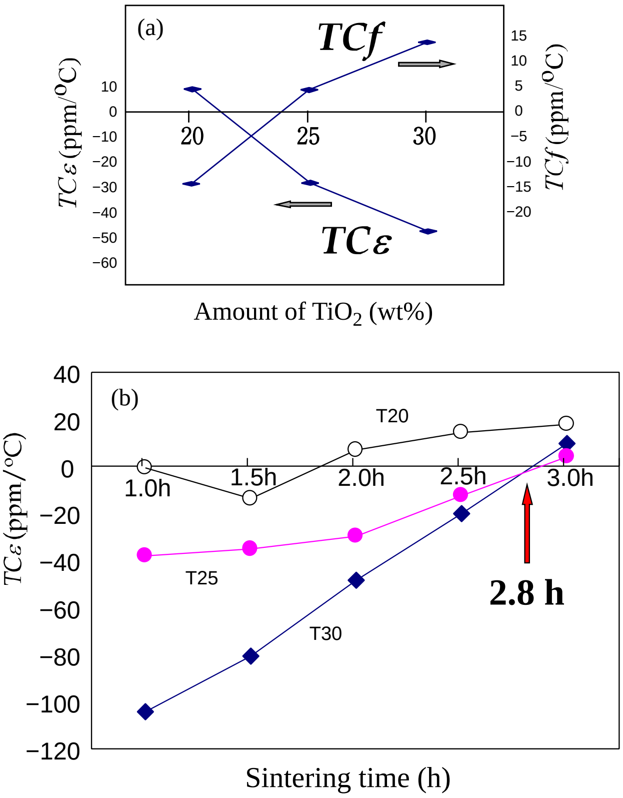

Fig. 5. (Color online) (a) Relationship between TCf and $TC\varepsilon$ as a function of amount of rutile added. (b) $TC\varepsilon$ of forsterite with rutile added, and sintered at 1200 °C as a function of sintering time. The arrow for 2.8 h shows the points of $TC\varepsilon = 0$ ppm/°C for T30 and T25.

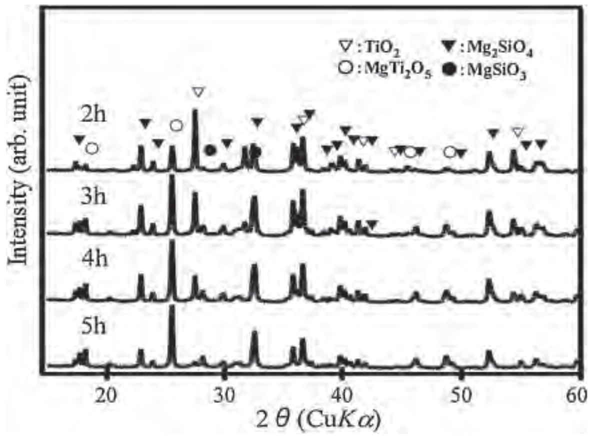

Fig. 6. XRPD patterns of forsterite with rutile added and sintered at 1200 °C for 2 to 5 h.

The decrease in TCf and increase in $TC\varepsilon$ depend on the amount of rutile, as shown in the reaction formula (1). Figure 6 shows the XRPD patterns of forsterite with 30 wt % rutile added and sintered at 1200 °C from 2 to 5 h.[23] The sintering time is prolonged from 3 to 5 h, because the decrease in the amount of rutile is not significant in the range from 2 to 3 h. The amounts of the rutile and $MgTi_2O_5$ phases indicated by open triangles and open circles decreased and increased, respectively, depending on the reaction formula (1). Finally, at 5 h of sintering, the rutile almost disappeared from the XRPD pattern. The forsterite and enstatite phases

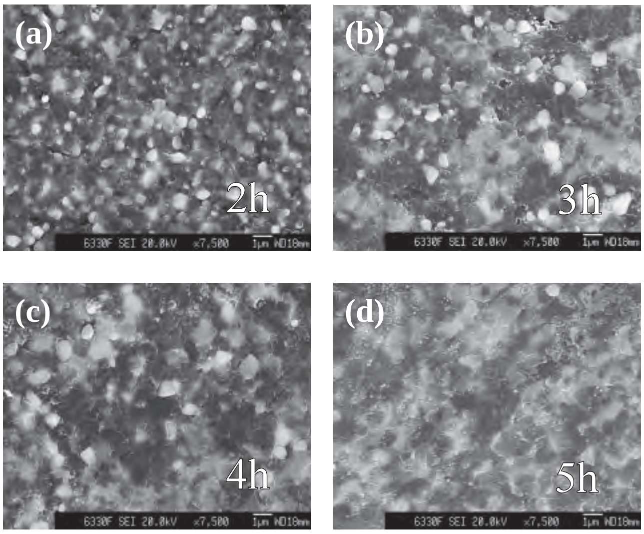

Fig. 7. Back-scatting electron images of forsterite with rutile added and sintered at 1200 °C for 2 to 5 h.

indicated by solid triangles and solid circles are decreased and increased, respectively, depending on the reaction formula (1). However, the decrease in the amount of forsterite is not so marked because of the large amount of forsterite. Figure 7 shows the back-scattering electron images of forsterite 30 wt% rutile added and sintered at 1200 °C from 2 to 5 h.[23] These are images of the samples with prolonged sintering time. The bright grains are rutile with high electron density. The brightness of certain areas decreases with sintering time, which indicating decreasing amount of rutile. In the images, the base material is forsterite, which reacted with rutile and converted to $MgTi_2O_5$ and enstatite. As the reactions are not very clear, the reaction process should be clarified to determine the role of rutile.

4. Conclusions

Zero ppm/°C *TCf* of forsterite with 30 and 25 wt% rutile added was achieved at 1200 °C and sintering time 2.5 and 2.25 h, respectively. The $TC\varepsilon$ of zero ppm/°C was also achieved for forsterite with 30 and 25 wt% rutile added at 1200 °C and sintering time of 2.8 h, and the $TC\varepsilon$ values for 20 wt% rutile added are ±15 ppm/°C. The ε_r values of the near-zero *TCf* forsterite with 30 and 25 wt% rutile added are 11.3 and 10.2, respectively. *TCf*, $TC\varepsilon$, and ε_r can be tuned on the basis of the data obtained. *Qf* was improved by the different procedures of samples such as powder formation technology and polishing the surface of the resonator.

Acknowledgments

The authors would like to thank Professors Ken-ichi Kakimoto and Isao Kagomiya of Nagoya Institute of Technology (NIT), Dr. Kensuke Wada of Toyota Central R&D Labs., Inc., Dr. Wilfried Wunderlich of Tokai University, Professors Hirotaka Ogawa and Akinori Kan of Meijyo University, Master Engineers Tomonori Sugiyama, Joshi Sugihara, Mio Terada, Yumi Inagaki, Yuuko Yamada, Kazuya Miwa, and Itaru Suzuki, who graduated from NIT, and Ms. Yasuko Sanma for support in typing. Part of this work was supported by the NEDO foundation for matching fund, A-step, and a Grant-in-Aid for Scientific Research from the Japan Society for the Promotion of Science. The late Project Professor Dr. Tsutomu Tsunooka studied millimeter-wave dielectrics of forsterite for 20 years. He discovered high-*Q* and zero-*TCf* forsterite. This study was performed under NEDO foundation for tuning the properties and stability of production for industrial mass production.

---

1) T. Tsunooka, H. Sugiura, Y. Higashida, T. Fukui, H. Okawa, and Y. Iwata: JFCC Rev. **4** (1992) 72 [in Japanese].
2) H. Ohsato: MRS Proc. **833** (2005) 55.
3) H. Ohsato, T. Tsunooka, M. Ando, Y. Ohishi, Y. Miyauchi, and K. Kakimoto: J. Korean Ceram. Soc. **40** (2003) 350.
4) M. T. Sebastian: *Dielectric Materials for Wireless Communication* (Elsevier, Amsterdam, 2008) p. 395.
5) I. Kagomiya, I. Suzuki, and H. Ohsato: Jpn. J. Appl. Phys. **48** (2009) 09KE02.
6) H. Ohsato, J.-S. Kim, A.-Y. Kim, C.-I. Cheon, and K.-W. Chae: Jpn. J. Appl. Phys. **50** (2011) 09NF01.
7) H. Ohsato, M. Terada, and K. Kawamura: Jpn. J. Appl. Phys. **51** (2012) 09LF02.
8) T. Tsunooka: Dr. Thesis, Faculty of Engineering, Nagoya Institute of Technology, Nagoya (2006) [in Japanese].
9) M. Andou, T. Tsunooka, Y. Higashida, H. Sugiura, and H. Ohsato: Abstr. Microwave Materials and Their Applications, 2002, p. 141.
10) T. Tsunooka, M. Ando, Y. Higashida, H. Sugiura, and H. Ohsato: J. Eur. Ceram. Soc. **23** (2003) 2573.
11) T. Tsunooka, H. Sugiyama, K. Kakimoto, H. Ohsato, and H. Ogawa: J. Ceram. Soc. Jpn. **112** (2004) S1637.
12) T. Tsunooka, T. Sugiyama, H. Ohsato, K. Kakimoto, M. Andou, Y. Higashida, and H. Sugiura: Key Eng. Mater. **269** (2004) 199.
13) T. Shimada and T. Tsunooka: Ceramics **39** (2004) 295 [in Japanese].
14) H. Ohsato, T. Tsunooka, T. Sugiyama, K. Kakimoto, and H. Ogawa: J. Electroceram. **17** (2006) 445.
15) Phase diagrams for ceramics No. 723, F. Massazza and E. Sirchia: Chim. Ind. (Milan) **40** (1958) 86.
16) M. Ando, H. Ohsato, I. Kagomiya, and T. Tsunooka: Jpn. J. Appl. Phys. **47** (2008) 7729.
17) M. Ando, K. Himura, T. Tsunooka, I. Kagomiya, and H. Ohsato: Jpn. J. Appl. Phys. **46** (2007) 7112.
18) B. W. Hakki and P. D. Coleman: IRE Trans. Microwave Theory Tech. **8** (1960) 402.
19) Y. Kobayashi and M. Katoh: IEEE Trans. Microwave Theory Tech. **33** (1985) 586.
20) T. Tsunooka: Electron. Ceram. **23** (1992) 29 [in Japanese].
21) T. Tsunooka: Ceramics **30** (1995) 309 [in Japanese].
22) M. Ando, H. Ohsato, and T. Tsunooka: Proc. 13th US-Japan Seminar on Dielectric and Piezoelectric Ceramics, 2007, p. 181.
23) Z. N. Ismarrubie, M. Ando, T. Tsunooka, I. Kagomiya, and H. Ohsato: Mater. Sci. Forum **561–565** (2007) 617.